JOURNAL OF SOLID STATE CHEMISTRY 33, 173–180 (1980)

The Factors Influencing Coordination Numbers in Solids

JEREMY K. BURDETT AND GUY L. ROSENTHAL

Department of Chemistry, The University of Chicago, Chicago, Illinois 60637

Received July 30, 1979; in final form September 20, 1979

An empirical plot of average principal quantum number ($\bar{n}$) versus average AX electronegativity difference ($\Delta\chi$) for A_nX_m structures shows resolution of four-, six-, and eight-coordinate solid state structures (Pearson diagrams). A simple molecular orbital (and therefore covalent) analysis of the coordination number problem suggests that it is determined by the balance between X–X nonbonded repulsions and the number of stabilizing interactions (both of which increase with coordination number). A–A repulsions may also be important if A is significantly larger than X. The approach provides an alternative to the ionic model for structure rationalization but it is still not clear how relatively important covalent and ionic factors are in determining the structures of even "ionic" solids.

Introduction

Traditional ways (*1*, *2*) of looking at solid state structures divide them into three types described by ionic, covalent, or metallic bonding. Materials of the first type are considered as being made up of discrete ions, the electrostatic forces between them holding the structure together. The predictive value of thermochemical, electrostatic lattice calculations using the ionic model is well established (*3*) (for "ionic" systems) but the use of traditional radius ratio rules to view the structures of the alkali halides and alkaline earth oxides, for example, predicts the correct room temperature/pressure structure with less than 50% accuracy (*4*). An empirical plot, however, of $\bar{n}$ versus $\Delta\chi$ (average principal quantum number of the A_nX_m formula unit, versus electronegativity difference between A and X) leads to well-defined areas where various types of structures are found (*5*). (We shall call these plots, Pearson diagrams.) Figure 1 presents results for some AX species and good resolution into four-coordinate sphalerite (zinc blende) and wurtzite, six-coordinate rock-salt, and

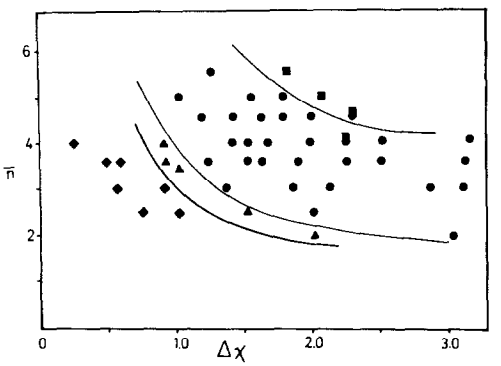

FIG. 1. A Pearson diagram showing observed stable room temperature/pressure polymorph for some AX systems. $\bar{n}$ is plotted against $\Delta\chi$ (average principal quantum number versus electronegativity difference between A and X). The AX species have a total of eight valence electrons per formula unit. Diamonds represent sphalerite (zinc blende) structure; triangles, wurtzite structure; (circles, rock-salt structure; squares, CsCl structure. (Adapted from Ref. (*5*).)

0022-4596/80/080173-08$02.00/0

eight-coordinate CsCl structures is found. Better agreement is found if instead of $\Delta\chi$, $\Delta\chi \cdot r_a/r_c$ is used as the ordinate, r_a and r_c are the anion and cation "radii," respectively. Interestingly, these plots resolve the two different four-coordinate structures. Similar features are seen for several A_nX_m structures. Higher coordination number structures are found (i) as the electronegativity difference increases and (ii) as the average principal quantum number increases. A separation between the structures of different coordination number is also found as a function of ionicity, measured experimentally via electronic absorption (*6*) or photoelectron (*7*) spectroscopic studies on solids. We have described elsewhere (*8*) how a covalent bonding model allows rationalization of the relative bond lengths in the wurtzite structure and why this structure appears to be favored compared to that of sphalerite for higher values of $\Delta\chi$ on the Pearson diagrams. In this paper we present molecular orbital arguments supported by quantitative calculations to rationalize the general appearance of the Pearson diagrams.

Covalent Factors Influencing Coordination Number

(a) *Nonbonded Repulsions*

1 shows the local coordination geometries of both "anion" and "cation" in the four-, six-, and eight-coordinate AX environments found in sphalerite and wurtzite, rock-salt, and CsCl structures, respectively. If we wish to retain the ligand–ligand distance pertaining to the four-coordinate complex in the higher coordination number structures, the A–X distance needs to be

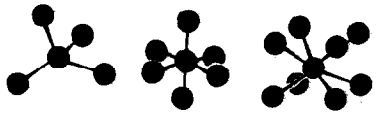

1

increased by 15.5% (in the AX_6 unit) and 41% (in the AX_8 unit), respectively. (The latter represents a 22% increase over the octahedral value.) These large changes in bond length with change of coordination number are seldom found (*9*). As a rule of thumb, "ionic" radii (and hence "bond length") should (*10*) depend upon coordination number in the approximate ratio 0.96 : 1.00 : 1.04 for four, six, and eight coordination. This implies that in real structures a decrease in ligand–ligand distance occurs with a concurrent increase in nonbonded repulsions as the coordination number increases. High coordination number structures are therefore only found with large central atoms so that there is sufficient "space" for the ligands in the coordination sphere.

(b) *Change in AX Bond Length*

Since the bond lengths in the y-coordinate geometries increase with coordination number, then it is likely that the interaction between the orbitals of A and X will decrease as y increases simply because of loss of overlap at the longer distance (*11*). Clearly factors (a) and (b) discourage the formation of high coordination numbers.

(c) *Change in the Number of Ligands*

In very simple terms, the more occupied ligand orbitals surrounding a central atom, the larger the stabilization energy associated with the interaction. Figure 2 shows molecular orbital diagrams for the three AX_y environments. In terms of second-order perturbation theory the changes in energy levels are pairwise additive (*12*). Thus the interaction energy of the totally symmetric central atom s orbital with the ligands is obtained by considering how it interacts with ligand 1, then linearly adding on to that how it interacts with ligand 2, etc. Using second- and fourth-order perturbation theory we may readily show (*13*) that in general the energy of interac-

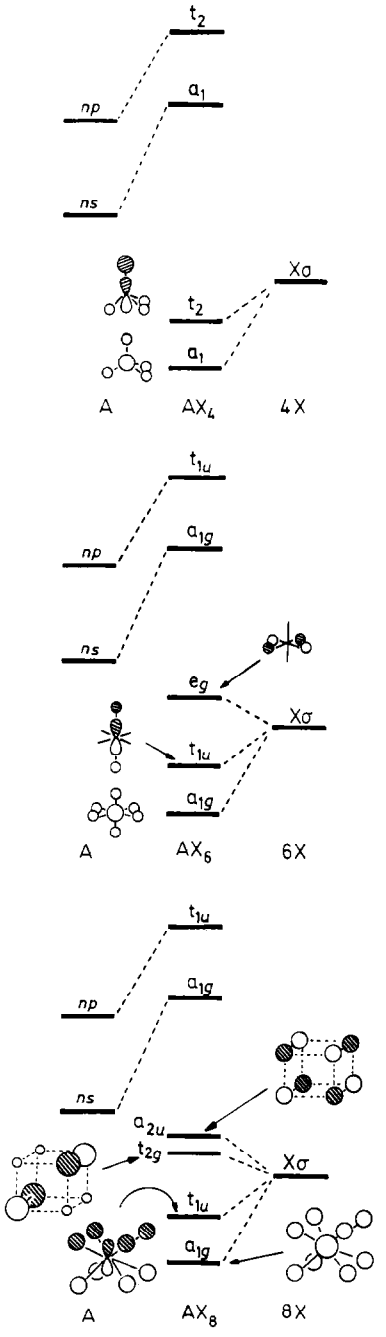

FIG. 2. σ-Only molecular orbital diagrams for AX_y units (y = 4, 6, 8) where the A atom is less electronegative than the X atoms. Only one component of degenerate orbitals is shown pictorially. The diagrams are schematic.

tion between two orbitals i and j is given by

$$\epsilon = p\beta_\lambda S_{\lambda 2} - p^2\lambda_\lambda S_\lambda^4,$$

where β_λ and γ_λ contain a dependence on the unperturbed energy separation between orbitals i and j, and p contains the dependence on the geometry and the number of ligands. S_λ is the overlap integral at a given AX distance between A and X orbitals of $\lambda(=\sigma, \pi)$ type. For the specific cases of Fig. 2, the total stabilization energy produced by occupation of the four A–X bonding orbitals is

$$2y[\beta_\sigma S_\sigma^2 + \beta'_\sigma S'^2_\sigma - y(\gamma_\sigma S_\sigma^4 + \tfrac{1}{3}\gamma'_\sigma S'^4_\sigma)].$$

Here y is the number of ligands (four, six, eight) and the unprimed and primed terms refer to interactions with the central atom s and p orbitals, respectivley. Division of this expression by y leads to the stabilization energy per A–X linkage,

$$2[\beta_\sigma S_\sigma^2 + \beta'_\sigma S'^2_\sigma - y(\gamma_\sigma S_\sigma^4 + \tfrac{1}{3}\gamma'_\sigma S'^4_\sigma)].$$

This decreases with increasing y. While the bonds in AX_4 might be regarded as $2c$–$2e$ bonds, those in AX_6 species would be of the weaker $3c$–$4e$ type as algebraically suggested here. The total stabilization energy (for a given bond length) does not increase lnearly with y, but as long as the fourth-order perturbation terms are smaller than the second-order terms, the total stabilization energy will increase with coordination number.

Generation of Pearson Diagrams

We have performed extended Hückel molecular orbital (EMHO) calculations on AX_y^{1-y} species, to test the importance of the three factors of the previous sections. (The detailed parameters and bond lengths are given in the Appendix.) Although crude in numerical terms compared to many quantum molecular calculations, the results do lead to a Pearson-like diagram. For the

AX_6 system of Fig. 2, the stabilization of the occupied A–X σ bonding orbitals of a_{1g} and t_{1u} symmetry (which in the a_{1g} case is also X–X bonding) is offset by the destabilization experienced by the A–X nonbonding, but X–X antibonding orbitals, of e_g symmetry. (See Fig. 2 for a pictorial representation of these orbitals.) In the AX_8 system, the stabilization of the occupied a_{1g} and t_{1u} orbitals is offset by the destabilization of the occupied X–X antibonding (and A–X nonbonding) orbitals of a_{2u} and t_{2g} symmetry. Occupation of these higher-energy X–X orbitals energetically gives rise to a nonbonded repulsion between the X atoms. The X atoms are closer together in the cubal coordination than in the octahedral environment and the net destablization energy associated with occupation of the a_{2u} and t_{2g} orbitals is greater than that associated with occupation of the e_g pair. From the numerical calculations we find that as the Slater exponent, ζ, of the orbitals on X increases (i.e., as the orbitals contract and X becomes more electronegative) (*14*) the destabilization of these X–X antibonding orbitals is reduced. With increasing ζ, the overlap integrals between ligand orbitals decrease faster than those between A and X. For $\bar{n} = 2$, by calculating the molecular orbital energy of AX_y^{1-y} relative to X_y^{-y} for each of the structures, AX_4 is found to be most stable for low values of ζ, AX_6 most stable for intermediate values, and AX_8 most stable for higher ζ values (Fig. 3). In qualitative terms this is just what is found in horizontal excurisons across the Pearson diagrams. Consideration only of the variation of A–X forces (we chose y times the bond overlap population) in these AX_y structures leads to the prediction of octahedral structures for low ζ and cubal structures for higher values. By viewing the energies of electrons in the σ bonding orbitals only (i.e., neglecting the effect of occupied X–X antibonding orbitals) the cubal structure is predicted to be most stable for all the values of ζ we used. These A–X σ bonding orbitals are also X–X bonding and their occupation will lead therefore to some X–X attraction. These three results for the $\bar{n} = 2$ cases strongly suggest that the coordination number in a given species is largely determined by factors (a) and (c) above.

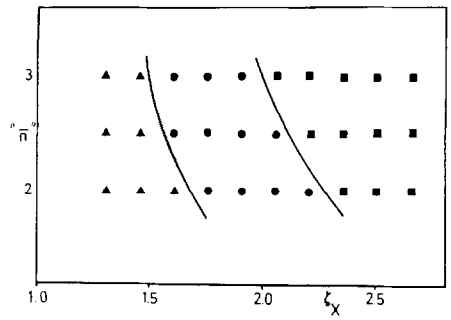

FIG. 3. Pearson diagram synthesized from the results of EHMO calcualtions on these AX_y^{1-y} species (see Appendix for details).

It will be noted in both Figs. 1 and 3 that the boundary between four- and six-, and between six- and eight-coordinate structures moves progressively to lower $\Delta\chi$ values as $\bar{n}$ increases. This is due in part to longer AX distances in general (*16*) as $\bar{n}$ increases with a concomitant increase in nonbonded X–X distances. The destabilizing effect of the occupation of X–X antibonding orbitals in AX_6 and AX_8 structures, with a given ζ is reduced compared with that in analogous structures with shorter A–X bond lengths. The higher coordination numbers then become more favorable. In addition, at the longer A–X distances, there are smaller changes between the A–X overlap integrals found at the distances appropriate for four, six, and eight coordination than for lower $\bar{n}$ systems (*17*). There is also a smaller effect via variation in the central atom exponent as heavier atoms are used.

A–A Repulsions

We have modeled the behavior in complex real systems by a simple molecular orbital model. Clearly, in any one specific case good-quality molecular orbital calculations should be used to reliably weigh the factors we have discussed above. Our EHMO calculations on LiF_y^{1-y} species (to model the LiF system), for example, using parameters commonly used for Li and F predict tetrahedral coordination, rather than the octahedrally based rock-salt structure found under normal conditions. Interestingly calculations on FLi_y^{+y-1} species show very little difference in energy among the three geometries. In these species (Fig. 4) the Li–Li antibonding orbitals are unoccupied and thus Li–Li nonbonded repulsions are absent on our model. This result suggests that it is X–X repulsions which most strongly influence the structure. O'Keefe and Hyde (*18*), however, in their molecular mechanics approach to four- and six-coordinate structures, suggested that it was cation–cation hard-sphere repulsions which determined the structure and not anion–anion repulsions as indicated by our molecular orbital results. The answer to this problem is that hard-sphere A–A repulsions may be important if there is a large difference in size between A and X. Obviously, oxygen, eight-coordinated by a large atom such as La, is unlikely because of effects of this sort. In this light recall that better resolution of structure on the Pearson diagrams is found (*5*) if $\Delta\chi \cdot r_a/r_c$ is used as the ordinate rather than $\Delta\chi$ alone. For large cation/small anion systems this modification means that lower coordination number structures are to be expected than predicted on $\Delta\chi$ grounds alone. Our valence molecular orbital model would not reflect effects of this sort. The modified ordinate thus contains the effects of A–A, X–X, and A–X forces in determining the structure.

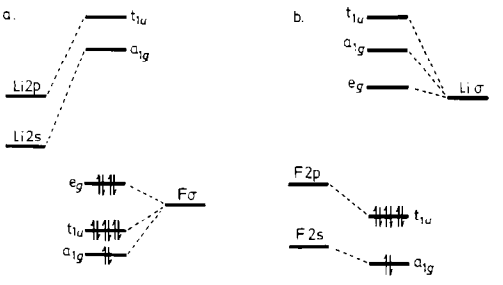

FIG. 4. Molecular orbital diagrams for (a) LiF_6^{-5} and (b) FLi_6^{+5} showing occupation of F–F antibonding orbitals in (a) but no occupation of Li–Li antibonding orbitals in (b). In this coordination geometry the X–X antibonding orbitals are those of species e_g. σ interactions only are shown for clarity on this schematic picture.

The Ionic Model

One inference often drawn from the Pearson diagrams is that as the electronegativity difference and average principal quantum number increase then the directional character of the bonds decreases and the bonding becomes omnidirectional. This is often regarded, if $\Delta\chi$ is large enough, as being due to ionic bonding. Our present analysis indicates that directional bonding occurs in all parts of the diagram. It immediately suggests a possible reason for the failure of the radius ratio rules in the alkali halides and alkaline earth oxides, namely, covalent bonding. This is an idea which is not new (*19*) but is formulated here in a rather different way. On an ionic model, a vertical section through the Pearson diagram is understandable. More highly coordinate structures are predicted as $\bar{n}$ increases. With the larger X–X distances, reduced electrostatic repulsions between the ligands will occur. On a local basis ionic repulsions between the X species increase as the charge on X increases (i.e., as $\Delta\chi$ increases) with a horizontal traverse across the dia-

gram, which should discourage the formation of high coordination numbers. This increase in X–X repulsions needs to be weighted against the increase in A–X attractions and the change in A–X distance. In the extended crystal the Madelung constants increase in the order sphalerite (1.638) < wurtzite (1.641) < rock salt (1.748) < CsCl (1.763). So the covalent factors (a–c) described above have their ionic analogs which give rise to similar effects. We can in fact calculate an approximate electrostatic energy for these structures as a function of ζ in a crude fashion by using the results of a population analysis of the molecular orbital coefficients. The parameter q_+q_-M/r_y is readily computed, where q_+ are the net atomic changes on anion and cations, r_y is their separation, and M is the Madelung constant for a given structure. As a general result q_- is similar for all three AX_y^{1-y} species with a given ζ but q_+ decreases in magnitude as y increases. For $n = 2$ wurtzite/sphalerite is most stable for all ζ considered but the energy difference between four and six coordination is much smaller for higher than for lower values of ζ. For $n = 3$ the net charges are much closer to unity. We find that wurtzite/sphalerite is most stable for values of ζ up to about 2.0 and that the rock-salt arrangement is more stable beyond. The CsCl structure is never the most stable structure on our scheme since the difference in r_y on going from six to eight coordination is always larger than the corresponding change in M.

Calculations to predict coordination number and crystal type have been performed by Tossell (*20*) using the modified electron gas (MEG) ionic model (*21*). The correct structures are predicted for MgF_2 (rutile) and CaF_2 (fluorite) but the method quantitatively starts to break down in predicting the correct coordination geometry (and also in predicting phase transition pressures) when systems are studied which do not have the highest possible ionic character (e.g., chlorides).

It is very interesting to note in this context that in the alkaline earth dihalides the AX_2 species with the largest electronegativity differences between A and X are nonlinear and those with the smallest differences are linear (*22*). Clearly on a purely ionic model, linear AX_2 species are strongly predicted. In the fluoride series, the linear molecules BeF_2 and MgF_2 have the geometry expected from the Walsh scheme and the VSEPR rules but the bent species CaF_2, SrF_2, and BaF_2 do not. Tossell's ionic calculations also do not predict these bent structures but their geometries are understandable in molecular orbital terms (*23*). The observed nonlinear structures for these heavy fluorides (in just those cases where ionic forces should be most important and linear geometries found) are clear evidence of the superiority of covalent over ionic forces in determining the *angular* geometry (at least). It is interesting to speculate that it is the covalent effects that dominate the coordination number problem outlined in this paper too.

Appendix: Molecular Orbital Parameters

EHMO calculations (*24*) were performed on AX_y^{1-y} species ($y = 4, 6, 8$). *ns* and *np* orbitals were included on A but 1*s* orbitals only on X to model the σ orbitals of the ligands. AX bond lengths for the three structures were in the ratio 0.96 : 1.00 : 1.04 for tetrahedral, octahedral, and cubal geometries, respectively. X atom orbital exponents ζ and valence shell ionization potentials in electron volts were varied according to the formula VSIP = 7.3ζ-1.0, the equation linking the parameters for the first-row species Li through F. The A atom exponents, VSIPs, and AX distances used to model variations in $\bar{n}$ are given in Table I. For the calculations on LiF, the octahedral Li–F distance used was 1.547 Å and

TABLE I

A ATOM EXPONENTS, VSIPS, AND *AX* DISTANCES

A	*n*	*ns,np* exponent	VSIP (*ns*) (eV)	VSIP (*np*) (eV)	*AX*(Å) (oct)
"Mg"	3	0.950	−9.00	−4.50	1.50
"Ca"	4	0.770	−7.20	−3.60	1.65
"Sr"	5	0.713	−6.70	−3.35	1.80

the VSIPs (with exponents in parentheses) were Li2*s*,5.40 (0.650); Li2*p*,3.50 (0.650); F2*s*,40.0 (2.600); F2*p*,18.1 (2.600).

Acknowledgments

We thank the Dreyfus Foundation for a Summer Fellowship (to G.L.R.) and Dr. J. A. Tossell for the results of his calculations prior to publication.

References

1. L. PAULING, "The Nature of the Chemical Bond," 3rd ed., Cornell Univ. Press, Ithaca, N.Y. (1960).
2. R. C. EVANS, "Crystal Chemistry," 2nd ed., Cambridge Univ. Press, New York/London (1964).
3. (*a*) A. F. KAPUSTINSKII, *Quart. Rev. Chem. Soc.* **10**, 283 (1956).
(*b*) T. C. WADDINGTON, *Advan. Inorg. Chem. Radiochem.* **1**, 157 (1959).
(*c*) D. A. JOHNSON, "Thermodynamic Aspects of Inorganic Chemistry," Cambridge Univ. Press, New York/London (1968).
4. (*a*) J. C. PHILLIPS (p. 1) AND W. B. PEARSON (p. 115), *in* "Treatise on Solid State Chemistry" (N. B. Hannay, Ed.), Vol. 1, Plenum, New York (1974).
(*b*) J. E. HUHEEY, "Inorganic Chemistry," 2nd ed., Harper & Row, New York (1978).
5. (*a*) E. MOOSER AND W. B. PEARSON, *Acta Crystallogr.* **12**, 1015 (1959).
(*b*) W. B. PEARSON, *J. Phys. Chem. Solids* **23**, 103 (1962).
6. J. C. PHILLIPS, *Rev. Mod. Phys.* **42**, 317 (1970).
7. S. P. KOWALCZYK, L. LEY, F. R. MCFEELY, AND D. A. SHIRLEY, *J. Chem. Phys.* **61**, 2850 (1974).
8. J. K. BURDETT, *J. Amer. Chem. Soc*, **102**, 450 (1980).
9. A table of "radii" as a function of coordination number was compiled by Huheey (see Ref. (*4b*). Small cations, e.g., Li^+ have a larger radius change with coordination number than anions, e.g., F^-.
10. J. D. DUNITZ AND L. E. ORGEL, *Advan. Inorg. Chem. Radiochem.* **2**, 1 (1960).
11. Tables of overlap integrals between Slater orbitals on different atoms as a function of orbital exponent and internuclear distance are given by : R. S. MULLIKEN, C. A. RIEKE, D. ORLOFF, AND H. ORLOFF, *J. Chem. Phys.* **17**, 1248 (1949).
12. R. HOFFMANN, *Accounts Chem. Res.* **4**, 1 (1971).
13. J. K. BURDETT AND T. A. ALBRIGHT, *Inorg. Chem.* **18**, 2112 (1979).
14. According to Slater's recipe, ζ is given by Z^*/n^* where Z^* is the effective nuclear charge seen by an electron in the orbital concerned and n^* an effective principal quantum number. The Allred–Rochow (see Ref. (*215*)) electronegativity (χ_{AR}) is related to Z^* in the following way:

$$\chi_{AR} = 0.359\,(Z^* + 0.35)/r^2 + 0.744,$$

where r is the covalent radius of the atom.
15. A. L. ALLRED AND E. G. ROCHOW, *J. Inorg. Nucl. Chem.* **5**, 264 (1958).
16. There is a compilation of some typical internuclear distances in Ref. (*4b*).
17. This result is presented with some reservations. We are at the mercy of the performance of the Slater orbitals.
18. M. O'KEEFE AND B. G. HYDE, *Acta Crystallogr. Sect. B.* **34**, 3519 (1978).
19. See, for example, a series of papers by Phillips and Van Vechten.
(*a*) J. C. PHILLIPS, *Phys. Rev. Lett.* **22**, 645 (1969).
(*b*) J. C. PHILLIPS AND J. A. VAN VECHTEN, *Phys Rev. Lett.* **22**, 705 (1969).
(*c*) J. C. PHILLIPS, *Science* **169**, 1035 (1970).
(*d*) J. C. PHILLIPS, "Covalent Bonding in Crystals, Molecules and Polymers," Univ. of Chicago Press, Chicago (1969).
20. J. A. TOSSELL, *J. Geophys. Res.* (in press).
21. R. G. GORDON AND Y. S. KIM, *J. Chem. Phys.* **56**, 3122 (1972).
22. V. CALDER, D. E. MANN, K. S. SESHADRI, M.

ALLAVENA, AND D. WHITE, *J. Chem. Phys.* **51,** 2093 (1969).
23. M. B. HALL, *Inorg. Chem.* **17,** 2261 (1978).
24. R. HOFFMANN, *J. Chem. Phys.* **39,** 1397 (1963); R. HOFFMANN AND W. N. LIPSCOMB, *J. Chem. Phys.* **36,** 3179 (1962), **37,** 2872 (1962).